Bioorganic & Medicinal Chemistry 21 (2013) 283–294

Contents lists available at SciVerse ScienceDirect

Bioorganic & Medicinal Chemistry

journal homepage: www.elsevier.com/locate/bmc

Pyrazolo[1,5-*c*]quinazoline derivatives and their simplified analogues as adenosine receptor antagonists: Synthesis, structure–affinity relationships and molecular modeling studies

Daniela Catarzi [a,*], Vittoria Colotta [a], Flavia Varano [a], Daniela Poli [a], Lucia Squarcialupi [a], Guido Filacchioni [a], Katia Varani [b], Fabrizio Vincenzi [b], Pier Andrea Borea [b], Diego Dal Ben [c], Catia Lambertucci [c], Gloria Cristalli [c]

[a] *Dipartimento di Scienze Farmaceutiche, Laboratorio di Progettazione, Sintesi e Studio di Eterocicli Biologicamente Attivi, Universita' di Firenze, Polo Scientifico, Via Ugo Schiff 6, 50019 Sesto Fiorentino, FI, Italy*

[b] *Dipartimento di Medicina Clinica e Sperimentale, Sezione di Farmacologia, Università di Ferrara, Via Fossato di Mortara 17-19, 44100 Ferrara, Italy*

[c] *School of Pharmacy, Medicinal Chemistry Unit, University of Camerino, Via S. Agostino 1, 62032 Camerino (MC), Italy*

ARTICLE INFO

Article history:
Received 5 September 2012
Revised 3 October 2012
Accepted 14 October 2012
Available online 29 October 2012

Keywords:
G protein-coupled receptors
Adenosine receptor antagonists
Pyrazoloquinazolines
Tricyclic heteroaromatic systems
Ligand–receptor modeling studies

ABSTRACT

A number of 5-oxo-pyrazolo[1,5-*c*]quinazolines (series **B-1**), bearing at position-2 the claimed (hetero)aryl moiety (compounds **1**–**8**) but also a carboxylate group (**9**–**14**), were designed as hA_3 AR antagonists. This study produced some interesting compounds endowed with good hA_3 receptor affinity and high selectivity, being totally inactive at all the other AR subtypes. In contrast, the corresponding 5-ammino derivatives (series **B-2**) do not bind or bind with very low affinity at the hA_3 AR, the only exception being the 5-*N*-benzoyl compound **19** that shows a hA_3 K_i value in the high μ-molar range. Evaluation of the synthetic intermediates led to the identification of some 5(3)-(2-aminophenyl)-3(5)-(hetero)arylpyrazoles **20**–**24** with modest affinity but high selectivity toward the hA_3 AR subtype. Molecular docking of the herein reported tricyclic and simplified derivatives was carried out to depict their hypothetical binding mode to our model of hA_3 receptor.

© 2012 Elsevier Ltd. All rights reserved.

1. Introduction

Adenosine is an endogenous nucleoside that plays a key role in different pathophysiological conditions by interacting with specific cell-surface G protein-coupled receptors (GPCRs) which are termed A_1, A_{2A}, A_{2B} and A_3 adenosine receptors (ARs).[1] Each receptor subtype mediates distinct physiological actions by coupling with different secondary messenger systems, such as adenylate cyclase (AC), calcium or potassium channels, phospholipase C and D. However, AC is considered the principal effector system which can be either inhibited (A_1 and A_3) or stimulated (A_{2A} and A_{2B}) thus decreasing or increasing, respectively, the cAMP production.[1–3] Due to the widespread distribution of ARs in peripheral organs and in the central nervous system (CNS),[1,3] and to the ubiquity of the natural ligand adenosine, selective modulation of each receptor subtype could be exploited for some therapeutic advantages. ARs have been recently recognized as novel and potential drug targets for therapeutic intervention in many pathological conditions such as cardiac and cerebral ischemia, asthma, renal failure, CNS disorders, inflammatory and neurodegenerative diseases.[4] Modulation of A_3 AR subtype has recently emerged as particularly interesting for the selective control of acute and chronic disorders such as cerebral and cardiac ischemia,[5,6] inflammation, and normal and tumor cell regulation.[7,8] Consequently, highly selective A_3 AR antagonists have been proposed for the acute treatment of stroke and for the development of cerebroprotective and anti-inflammatory drugs. The potential use of A_3 AR antagonists as therapeutics in cancers is still under debate.[7]

The putative therapeutic applications of A_3 AR antagonists as well as the growing need for pharmacological tools to deeply investigate A_3 AR roles, has made the identification of potent and selective antagonists at this receptor subtype, endowed with adequate pharmacokinetic properties, an emerging topic.

Our research group has developed several classes of tricyclic AR antagonists[6,9–16] including the 2-arylpyrazolo[3,4-*c*]quinoline series (**PQ**)[6,12–14] (Fig. 1). By modulating substituents at positions 2 and 4 of this scaffold, we have obtained highly potent and selective hA_3 AR antagonists.[6,12,13] Structure–activity relationships (SAR) of these derivatives showed that the 2-aryl-4-oxo-substituted compounds (**Series A-1**) have, on the whole, a higher affinity for the hA_3 AR[6,12] than the corresponding 4-amino derivatives (**Series A-2**).[12]Interestingly, the hA_3 receptor affinities of the 2-arylpyrazolo[3,4-*c*]quinolin-4-amines were enhanced when acyl

* Corresponding author. Tel.: +39 055 4573722; fax: +39 055 4573780.
E-mail address: daniela.catarzi@unifi.it (D. Catarzi).

0968-0896/$ - see front matter © 2012 Elsevier Ltd. All rights reserved.
http://dx.doi.org/10.1016/j.bmc.2012.10.031

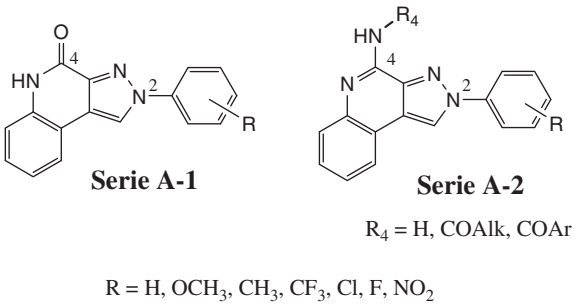

Figure 1. Previously reported pyrazolo[3,4-*c*]quinoline (**PQ**) derivatives as hA_3 adenosine receptor antagonists.

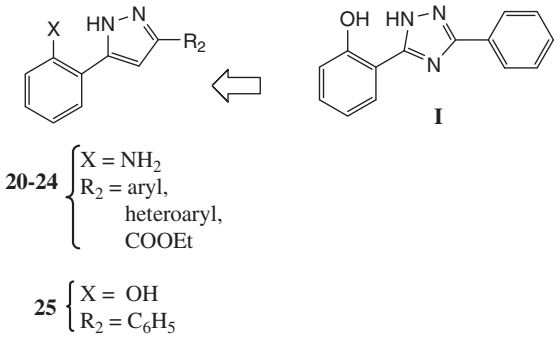

Figure 3. Simplified adenosine receptor antagonists: 3,5-Diarylpyrazole derivatives.

residues were appended on the 4-amino group.[6,12,13] Moreover, in both the 4-oxo- (**A-1**) and 4-amino (**A-2**) series the presence of a methoxy substituent at the *para*-position of the 2-phenyl ring ameliorated the hA_3 AR binding affinity.[6,12] The SAR on these pyrazoloquinolines resemble those of other classes of tricyclic AR antagonists which were extensively studied in our laboratory.[9,10,15,16] On this basis, we have designed a new series of pyrazolo[1,5-*c*]quinazoline derivatives differently substituted at position-2 and 5 (**Series B-1** and **B-2**, Fig. 2). The present study was performed to evaluate the versatility of the pirazoloquinazoline scaffold to obtain new potent and selective AR antagonists.

Together with the classical 5-oxo- and 5-amino- patterns, different aryl, heteroaryl and carboxyalkyl substituents were introduced at position-2 of the tricyclic ring system. These modifications were performed on the basis of the SARs on structurally correlated AR antagonists synthesized in our laboratory.[6,12,13,15,16] Moreover, our attention was also addressed to the development of more simplified heterocyclic compounds.[17–19] In fact, structural simplification can represent a drug design strategy to shorten the synthetic route and to improve physicochemical properties of the original candidate. Thus, looking at the intermediates in the synthetic pathway which leads to the pyrazolo[1,5-*c*]quinazoline derivatives, we have identified the 3(5)-(2-aminophenyl)-5(3)-(hetero)aryl-pyrazoles **20–24**[20,21] (Fig. 3) as possible candidates for our pharmacological assays. In fact, these derivatives seem to have, on the whole, the minimal structural requirements (i.e., the primary amino group and the correctly oriented aryl moieties) to profitably interact with the AR binding pocket. The presence of the primary amino group is also important for solubility purposes, as is the polar pyrazole NH function. Moreover, other evidence prompted us to investigate in this direction. In fact, five-member monocyclic cores have been evaluated as AR antagonists[22] in recent years. Among them, our attention was caught by the 5-(2-hydroxyphenyl)-3-phenyl-1,2,4-triazole **I** (Fig. 3) which was reported as a weak hA_{2A} AR antagonist (K_i = 0.7 μM) together with other triazole derivatives.[23] In this regard, we also considered the corresponding 5-(2-hydroxyphenyl)-3-phenylpyrazole **25**[20] (Fig. 3) as a link between the 3(5)-substituted 5(3)-(2-aminophenyl)-pyrazole series **20–24** and the lead triazole **I**. In fact, the close structural similarities between these two different monocyclic scaffolds seem intriguing.

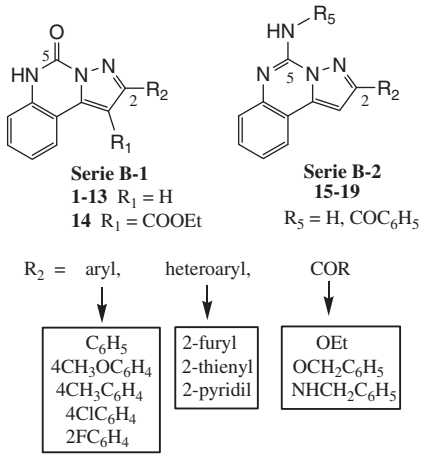

Figure 2. Currently reported pyrazolo[1,5-*c*]quinazoline derivatives.

2. Chemistry

The 5,6-dihydro-2-(hetero)arylpyrazolo[1,5-*c*]quinazolin-5-ones **1**, **3–5**, **8**, the alkyl 5,6-dihydro-5-oxo-pyrazolo[1,5-*c*]quinazolin-2-carboxylates **9–11**, together with the synthetic intermediates **20** and **24**, and the diethyl 5,6-dihydro-5-oxo-pyrazolo[1,5-*c*]quinazolin-1,2-dicarboxylate **14**, were synthesized as reported in previously published papers.[20,21,25] The synthesis of the 2-arylpyrazolo[1,5-*c*]quinazoline derivatives **2, 6–7, 15–19** and that of the 2-carboxy-substituted analogues **12–13** is depicted in Schemes 1 and 2, respectively. Preparation of compounds **6–7** was performed following different procedures with respect to those previously reported.[21]

By reacting commercially available 2-nitrobenzaldehyde with the suitable (hetero)aryl-methylketone in the presence of boron trifluoride acetic acid complex, in glacial acetic acid, the 1,3-diaryl-2-propenones **26–28**[26–28] were obtained with high yields (Scheme 1). The latters were then reacted with hydrazine hydrate yielding the 4,5-dihydro-3,5-diaryl-1*H*-pyrazoles **29–31**[21] which were dehydrogenated to the 3(5)-(2-nitrophenyl)-5(3)-(hetero)aryl-pyrazoles **32–34** by reaction with lead tetracetate followed by treatment with concentrated hydrochloric acid in boiling ethanol. Catalytic reduction of the nitro group of **32–34** afforded the corresponding amino derivatives **21–23**[21] which were cyclized to the tricyclic compounds 5-oxo- (**2**, **6–7**) and 5-amino- (**16–18**) substituted by reacting, respectively, with triphosgene and cyanamide. The tricyclic 2-phenyl-5-amino substituted derivative **15**, obtained by treating the 5-(2-aminophenyl)-3-phenyl-1,2,4-triazole **20**[20] with cyanamide, was reacted with benzoyl chloride in the presence of anhydrous pyridine to give the corresponding 5-benzamido compound **19**. Hydrolysis of the ethyl 5,6-dihydro-5-oxo-pyrazolo[1,5-*c*]quinazolin-2-carboxylate **10**[20] (Scheme 2) yielded the corresponding 2-carboxylic acid **35**[21] that was transformed into the 2-carbonyl chloride by reacting with an excess of thionyl chloride. The crude product was heated at reflux with benzyl alcohol to give the corresponding benzyl 2-carboxylate **12**. By reacting **35** with benzylamine in the presence of *N*-(3-dimethylaminopropyl)-*N*′-ethylcarbodiimide hydrochloride and 1-hydroxybenzotriazole hydrate, the 2-benzylcarboxamido derivative **13** was obtained.

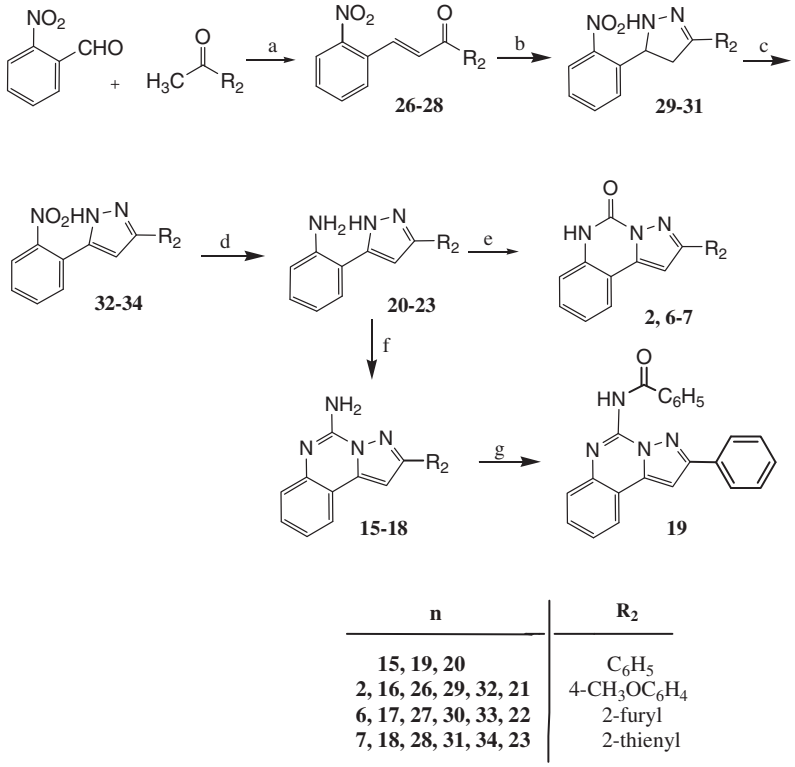

n	R_2
15, 19, 20	C_6H_5
2, 16, 26, 29, 32, 21	4-$CH_3OC_6H_4$
6, 17, 27, 30, 33, 22	2-furyl
7, 18, 28, 31, 34, 23	2-thienyl

Scheme 1. Synthesis of 2-arylpyrazolo[1,5-*c*]quinazoline derivatives. Reagents and conditions: (a) $BF_3{\cdot}(CH_3COOH)_2$, acetic acid, room temperature; (b) $NH_2NH_2{\cdot}H_2O$, EtOH, reflux; (c) (i) $Pb(OAc)_4$, anhydrous CH_2Cl_2, room temperature; (ii) conc. HCl, EtOH, reflux; (d) H_2, 10% Pd/C, EtOAc; (e) $(CCl_3O)_2CO$, anhydrous THF, room temperature; (f) NH_2CN, pTsOH, NMP, reflux; (g) C_6H_5COCl, anhydrous pyridine, anhydrous CH_2Cl_2, room temperature.

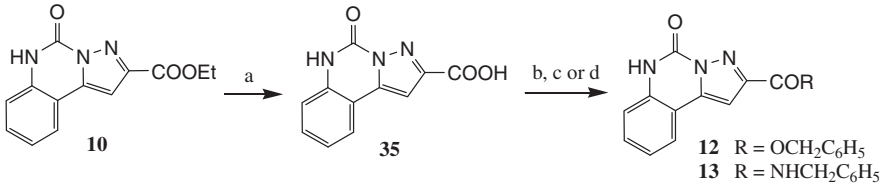

Scheme 2. Synthesis of 2-carboxy-substituted pyrazolo[1,5-*c*]quinazoline derivatives. Reagents and conditions. (a) 6N HCl, glacial acetic acid, reflux; (b) $SOCl_2$, reflux; (c) $C_6H_5CH_2OH$, reflux; (d) $C_6H_5CH_2NH_2$, *N*-(3-dimethylamino-propyl)-*N*′-ethylcarbodiimide·HCl, 1-hydroxybenzotriazole hydrate.

3. Pharmacology

All the reported compounds **1–25**, were tested for their ability to displace specific [^{3}H]DPCPX, [^{3}H]ZM241385 and [^{125}I]AB-MECA binding from cloned hA_1, hA_{2A} and hA_3 receptors, respectively, stably expressed in CHO cells. Compounds **1–25** were also tested at the hA_{2B} subtype by measuring their inhibitory effects on NECA-stimulated cAMP levels in CHO cells stably transfected with the hA_{2B} receptor. The results of binding experiments and cAMP assays in hA_{2B} CHO cells are reported in Tables 1 and 2, where hA_1, hA_{2A} and hA_3 affinities of **I** are also included as reference data. Moreover, to evaluate their hA_3 AR antagonistic effect, compounds **2**–**4**, **6** and **7** were tested for their ability to counteract the Cl-IB-MECA-mediated inhibition of cAMP production in CHO cells stably expressing hA_3 AR (Table 3).

4. Results and discussion

4.1. Structure–affinity relationships

The binding results reported in Tables 1 and 2 indicate that we have produced some new selective hA_3AR antagonists belonging to the pirazolo[1,5-*c*]quinazoline series **B-1** and **B-2**. In particular, while the 5-oxo-substituted derivatives (series **B-1**) are endowed with good hA_3 receptor affinity and selectivity, the corresponding 5-ammino compounds (series **B-2**) do not bind or bind with very low affinity at the same receptor subtype, the only exception being the 5-benzamido substituted derivative **19**. In contrast, the 4-amino compound **17**, bearing a 2-furyl moiety at position-2, is the only compound among series **B-1** and **B-2** which binds at all the hARs with the exception of the hA_3 subtype. Moreover, evaluation of the synthetic intermediates **20–24** for the binding at the hARs gave good results thus leading to some modest but selective hA_3 AR antagonists despite their highly simplified structure.

It has to be noted that both the 5-oxo and 5-amino derivatives **1** and **15**, respectively, bearing a phenyl substituent at position-2, are devoid of significant affinity toward all the human AR subtypes. This result was almost unexpected considering the close structural similarities between the pyrazolo[1,5-*c*]quinazoline scaffold and the pyrazolo[3,4-*c*]quinoline (**PQ**) core of the lead compounds (Fig. 1). In fact, all the structural features which are considered as essential for a profitable receptor–ligand interaction are present in both the 2-phenylpyrazolo[1,5-*c*]quinazoline either 5-oxo (**1**) or 5-amino (**15**) substituted. Replacement of the 2-phenyl group of **1**

Table 1
Binding affinity (K_i) at hA_1, hA_{2A}, and hA_3 ARs and potencies (IC_{50}) at hA_{2B}

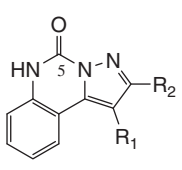

Series B-1 (1-14)

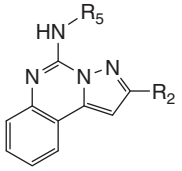

Series B-2 (15-19)

Series	n°	R_1	R_2	R_5	Binding experiments K_i[a] (nM) or *I*%			cAMP assay *I*%
					hA_3[b]	hA_1[c]	hA_{2A}[d]	hA_{2B}[e]
	1	H	C_6H_5	—	28%	12%	1%	4%
	2	H	4-$OCH_3C_6H_4$	—	100 ± 12	4%	1%	2%
	3	H	4-$CH_3C_6H_4$	—	25 ± 2	1%	12%	2%
	4	H	4-ClC_6H_4	—	23 ± 2	6%	1%	3%
	5	H	2-FC_6H_4	—	140 ± 16	1%	11%	1%
	6	H	2-Furyl	—	80 ± 7	5%	1%	3%
B-1	**7**	H	2-Thienyl	—	40 ± 3	7%	20%	6%
	8	H	2-Pyridil	—	252 ± 13	4%	1%	2%
	9	H	COOMe		440 ± 44	1%	3%	6%
	10	H	COOEt	—	315 ± 20	3%	5%	3%
	11	H	$COOCH(CH_3)_2$		450 ± 42	1%	1%	4%
	12	H	$COOCH_2C_6H_5$	—	1%	3%	4%	2%
	13	H	$CONHCH_2C_6H_5$	—	25%	2%	5%	1%
	14	COOEt	COOEt	—	101 ± 12	12%	1%	5%
	15	—	C_6H_5	NH_2	15%	1%	5%	3%
	16	—	4-$OCH_3C_6H_4$	NH_2	45%	7%	15%	3%
B-2	**17**	—	2-Furyl	NH_2	35%	35 ± 2	80 ± 7	120 ± 13
	18	—	2-Thienyl	NH_2	18%	44%	20%	3%
	19	—	C_6H_5	$NHCOC_6H_5$	520 ± 60	13%	1%	4%

[a] K_i values are means ± SEM of four separate assays each performed in duplicate. Percentage of inhibition (*I*%) are determined at 1 μM concentration of the tested compounds.
[b] Displacement of specific [^{125}I]AB-MECA competition binding to hA_3CHO cells.
[c] Displacement of specific [^{3}H]DPCPX competition binding to hA_1CHO cells.
[d] Displacement of specific [^{3}H]ZM241385 competition binding to hA_{2A}CHO cells.
[e] Percentage of inhibition on cAMP experiments in hA_{2B}CHO cells, stimulated by 200 nM NECA, at 1 μM concentration of the examined compounds.

Table 2
Binding affinity (K_i) at hA_1, hA_{2A}, and hA_3 ARs and potencies (IC_{50}) at hA_{2B} AR

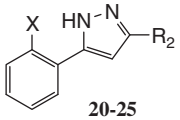

20-25

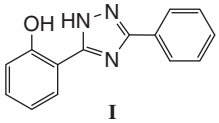

I

	R_2	X	Binding experiments K_i[a] (nM) or *I*%			cAMP assay *I*%
			hA_3[b]	hA_1[c] (%)	hA_{2A}[d] (%)	hA_{2B}[e] (%)
20	C_6H_5	NH_2	680 ± 62	9	1	2
21	4-$CH_3OC_6H_4$	NH_2	480 ± 53	2	9	5
22	2-Furyl	NH_2	1%	4	6	1
23	2-Thienyl	NH_2	600 ± 57	2	1	3
24	COOEt	NH_2	23%	3	1	2
25	C_6H_5	OH	7%	13	1	4
I[f]	—	—	39%	47	2	8

[a] K_i values are means ± SEM of four separate assays each performed in duplicate. Percentage of inhibition (*I*%) are determined at 1 μM concentration of the tested compounds.
[b] Displacement of specific [^{125}I]AB-MECA competition binding to hA_3CHO cells.
[c] Displacement of specific [^{3}H]DPCPX competition binding to hA_1CHO cells.
[d] Displacement of specific [^{3}H]ZM241385 competition binding to hA_{2A}CHO cells.
[e] Percentage of inhibition on cAMP experiments in hA_{2B}CHO cells, stimulated by 200 nM NECA, at 1 μM concentration of the examined compounds.
[f] Ref.[23,24]

with suitable moieties significantly reinforces the receptor–ligand interaction, thus leading to compounds **2–8** that possess enhanced hA_3 binding affinities. In particular, the ameliorated binding of the 2-(4-methoxyphenyl)-substituted compound **2**, with respect to the parent **1**, was expected on the basis of the lead SARs.[6,12] In fact, the 4-methoxy group could improve the receptor–ligand interaction by forming a weak hydrogen bond with a suitable receptor site[6] or by reinforcing the π–π stacking interaction of the 2-phenyl ring with the receptor, due to its electron-donating properties. The lipophilic contribution of the methoxy group to the ligand

Table 3
Potencies (IC_{50}) of some selected pyrazoloquinoline derivatives at hA_3AR

	cAMP assays hA_3 IC_{50} (nM)[a]
2	324 ± 32
3	88 ± 9
4	82 ± 8
6	138 ± 13
7	263 ± 25

[a] IC_{50} values represent the mean ± SEM of four separate cAMP experiments in hA_3 CHO cells, inhibited by 100 nM Cl-IB-MECA.

interaction is negligible. In contrast, introduction of either the 4-methyl or the 4-chloro substituent (compound **3** and **4**, respectively) strongly affected the hA_3 binding affinity probably by increasing the hydrophobic interactions at the level of the 2-phenyl substituent. Moreover, it is evident that introduction at position-2 of the pyrazoloquinazoline scaffold of a 2-fluorophenyl (compound **5**), 2-furyl (**6**), 2-thienyl (**7**) or 2-pyridil (**8**) moiety improves the hA_3 receptor–ligand interactions with respect to the parent **1**. This could be due to the presence, in the 2-substituent, of an heteroatom able to reinforce the binding with the receptor through a profitable hydrogen bond. The improved hA_3 binding affinity of the 5-oxo-substituted compounds **5–8** compared to the corresponding 2-phenyl derivative **1**, suggested introduction at position-2 of an alkyl carboxylate group (compounds **9–11**), that could ameliorate interaction with the receptor as hypothesized above for the 2-substituent of compounds **5–8**. As expected, compounds **9–11** are endowed with hA_3 binding affinity higher than that of the reference **1**, and comparable to that of the 2-pyridil compound **8**. The positive effect exerted by the alkyl 2-carboxylate groups on this scaffold prompted us to introduce at position-2 a benzyl-carboxylate ester and amide (compounds **12** and **13**, respectively) in order to increase hydrophobic interactions. Unfortunately, this modification does not positively affect the hA_3 affinity as observed in other series of tricyclic AR antagonists.[16] It is clear that the A_3 binding pocket which accommodates the 2-substituent has precise steric requirements, being compounds **12** and **13** completely inactive. In contrast, introduction of a further ethyl carboxylate function at position-1 of **10** yielded compound **14** which shows a three-fold enhanced hA_3 binding affinity with respect to that of the parent mono-substituted **10**. This result can be interpreted considering the presence at the receptor level of a cavity large enough to well accommodate this group.

However, although these new 5-oxo-pyrazoloquinazoline derivatives **1–14** do not possess very high hA_3 receptor affinity, they are, without any doubt, highly selective due to their total inactivity at all the other three AR subtypes.

The lower binding affinities of the 5-amino substituted derivatives **15–18** with respect to those of the corresponding 5-oxo compounds **1–2**, **6–7** was expected[12] even if not to such extent. However, the dramatic increase of the hA_{2A}, A_{2B} and A_1 binding affinities of the 5-amino-2-furyl derivative **17** with respect to those of the corresponding 2-phenyl one **15** confirms the profitable effect exerted by the presence of the 2-furyl ring. It is, however, difficult to explain not only the low or null hA_3 affinity of both the 2-(2-furyl) compound **17** and the corresponding 2-(2-thienyl) derivative **18**, but also the total discrepancy of binding results between **18** and **17** at the other AR subtypes. In fact, these data are not in accordance with those obtained on the 5-oxo-pyrazoloquinazoline **6**, **7** and on other tricyclic hA_3 AR antagonists.[16] To increase the hydrophobic interactions of these 5-amino derivatives with the receptor site, the 5-benzoylamino substituted derivative **19** was synthesized. An ameliorated hA_3 affinity was observed, which could be ascribed also to an additional hydrogen bond interactions of the 5-amide function with specific receptor sites.

Furthermore, the effect of compounds **2–4**, **6** and **7** in limiting the Cl-IB-MECA-inhibited cAMP accumulation in hA_3 CHO cells was determined. In accordance with their hA_3 affinity, all the selected pyrazoloquinoline derivatives proved to be very potent in this test, showing an antagonistic behavior (Table 3).

The results obtained up to now on these new tricyclic AR antagonists are, in our opinion, not so intriguing to encourage further investigation in such direction. However, we considered it very interesting to biologically evaluate the synthetic pyrazole intermediates **20–24**. These 3(5)-(2-aminophenyl)-5(3)-aryl-pyrazoles are closely correlate with the hA_{2A} AR antagonist 5-(2-hydroxyphenyl)-3-phenyl-1,2,4-triazole **I**[23,24] which was re-tested in our binding assays together with the pyrazole analogue 2-hydroxyphenyl substituted **25**.[20] Compound **I** turned out to be totally inactive at the hA_{2A} and hA_{2B} AR subtypes, while it shows *I*% values of 39 and 47, respectively, at the hA_3 and hA_1 subtypes, at 1 μM concentration. It has to be noted that our biological result on the hA_{2A} AR (I = 2%) is in total disagreement with that reported in the literature (K_i = 0.7 μM), but can be considered in accordance with the data obtained on the pyrazole analogue **25**.

Interestingly, despite the extreme structural simplification of these monocyclic compounds **20–24** with respect to the tricyclic derivatives **15–18**, some of them are endowed with hA_3 binding affinity in the μ-molar range and, more importantly, they have total selectivity, being completely inactive at all the other AR subtypes. However, the SAR obtained for these compounds do not resemble those of the pyrazoloquinolines herein reported. In fact, while the 3(5)-phenylpyrazole **20** is endowed with a hA_3 affinity in the high μ-molar range, the corresponding furyl substituted derivative **22** is totally inactive at the same receptor subtype. An opposite trend can be observed in the tricyclic series: the 2-phenyl substituted compound **1** is totally inactive at the hA_3 AR, while the 2-furyl substituted **6** shows high affinity and selectivity for this receptor subtype.

4.2. Molecular modeling studies

To define the structural features at the base of the different binding affinities of the new derivatives, a molecular docking analysis was performed on homology models of hA_3AR developed by using three recently published crystal structures of the $A_{2A}AR$ in complex with the ZM241385 antagonist as templates (PDB code: 3EML; 2.6-Å resolution;[29] PDB code: 3PWH; 3.3-Å resolution;[30] PDB code: 3VG9; 2.7-Å resolution[31]). The $A_{2A}AR$ crystal structure allows improvement of the accuracy of AR homology models, due to the high residue conservation in the primary sequences of the AR subtypes, which share a sequence identity of ~57% within the transmembrane (TM) domains.[32] The residues located within the seven TM domains in the upper part of ARs, corresponding to the ligand binding site, are conserved with an average identity of 71%.[33] Furthermore, the $A_{2A}AR$ crystal structure is solved in complex with the high affinity antagonist ZM241385, hence presenting a cavity suitable as binding site for docking analysis. The obtained hA_3AR homology models were checked by using the Protein Geometry Monitor application within MOE,[34] which provides a variety of stereochemical measurements for inspection of the structural quality in a given protein, such as backbone bond lengths, angles and dihedrals, Ramachandran φ–ψ dihedral plots, and sidechain rotamer and nonbonded contact quality.

Structures of hA_3AR were then used as target for the docking analysis of synthesized derivatives. All ligand structures were optimized using RHF/AM1 semi-empirical calculations and the software package MOPAC implemented in MOE was utilized for these calculations.[35] The compounds were then docked into the

binding site of the hA_3AR models by using the MOE Dock tool. Top-score docking poses of each compound were subjected to energy minimization and then rescored using three available methods implemented in MOE: the *London dG* scoring function that estimates the free energy of binding of the ligand from a given pose; the *Affinity dG* scoring tool that estimates the enthalpic contribution to the free energy of binding; the *dock-pK_i* predictor that uses the MOE scoring.svl script to estimate for each ligand a pK_i value, which is described by the H-bonds, transition metal interactions, and hydrophobic interactions energy. For each compound, the three top-score docking poses, according to at least two out of three scoring functions, were selected for final ligand–target interaction analysis.

The docking methodology was first tested by comparing the predicted binding mode of ZM241385 within the $A_{2A}AR$ pocket to the X-ray data. The docking method showed good ability to reproduce the ZM241385 binding mode observed in the experimental data. In particular, the RMSD from the comparison of the crystal structure and the docking conformation was calculated as 1.4547, 1.3302, and 2.7320 Å (for the 3EML, 3PWH, and 3VG9 crystal structure, respectively), with the best matching being given by the 2-(furan-2-yl)-[1,2,4]triazolo[1,5-*a*][1,3,5]triazin-7-amine moiety and the highest deviation being given by a slightly different orientation of the 4-(2-aminoethyl)phenol group.

The three hA_3AR models developed present highly similar binding sites by considering both pocket volumes and receptor residue orientation. In the binding pocket only subtle rearrangements of some flexible residues are observed, while higher conformational variability is observed at EL domains in peripheral regions of the binding site. As consequence, it is not a surprise that the docking analysis of the synthesized compounds at the three receptor models led to analogous results. Considering the general binding mode of the 5-oxo-substituted pyrazoloquinazoline derivatives in the hA_3AR, two main sets of docking conformations were observed with all three hA_3AR models. The first set of conformations (from this point on called 'family 1') are depicted in Figure 4 where compound **4** is shown as template. Family 1 conformations present the pyrazoloquinazoline moiety located approximately in correspondence

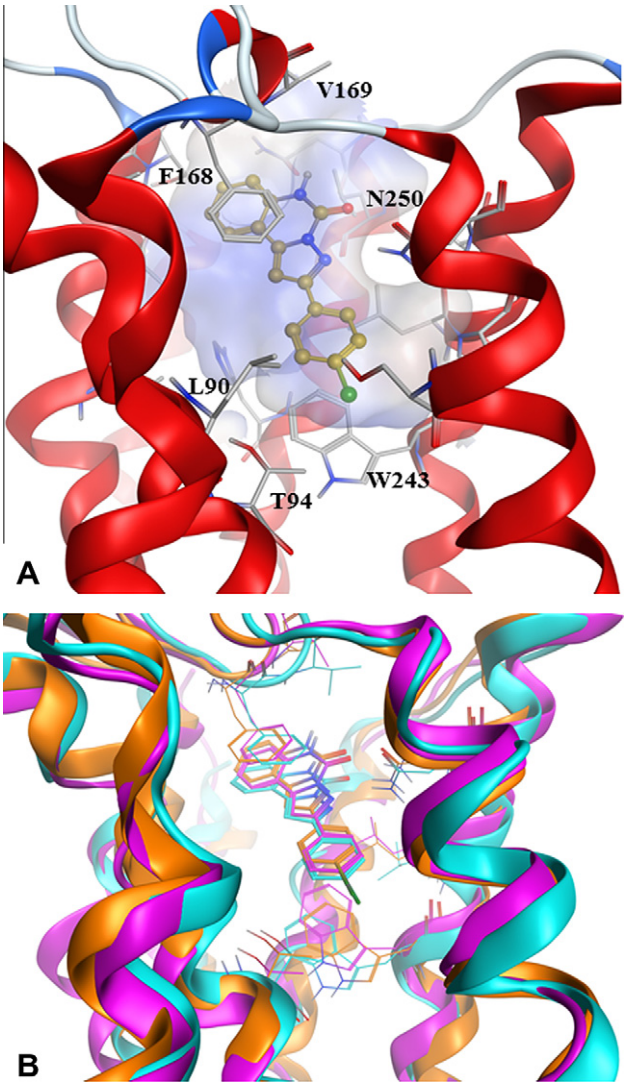

Figure 4. Panel A: Family 1 docking conformations, binding mode of compound **4** (yellow) at 3EML-based hA_3AR model is shown as example; key receptor residues are indicated. Panel B: Superimposition of the three hA_3AR models and docking conformations of compound **4**; 3EML-, 3PWH-, and 3VG9-based hA_3AR models are colored in orange, magenta, and cyan, respectively; docking conformations of compound **4** at the three receptor models are colored accordingly.

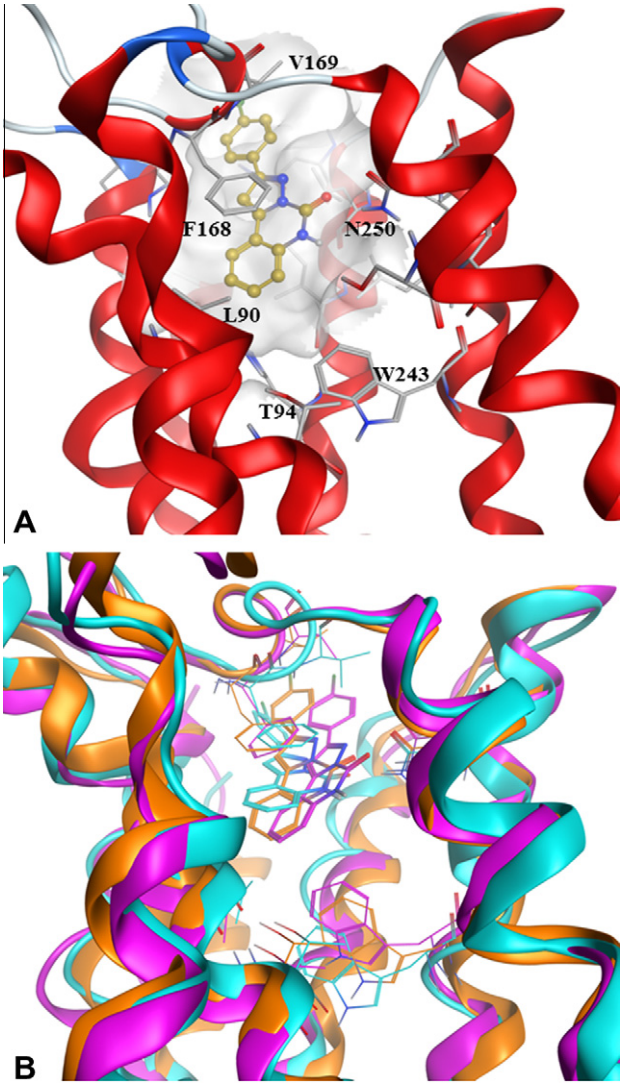

Figure 5. Panel A: Family 2 docking conformations, binding mode of compound **4** (yellow) at 3EML-based hA_3AR model is shown as example; key receptor residues are indicated. Panel B: Superimposition of the three hA_3AR models and docking conformations of compound **4**; 3EML-, 3PWH-, and 3VG9-based hA_3AR models are colored in orange, magenta, and cyan, respectively; docking conformations of compound **4** at the three receptor models are colored accordingly.

with the [1,2,4]triazolo[1,5-*a*][1,3,5]triazine scaffold of the co-crystallized ZM241385 antagonist. The 2-substituent is pointed towards the central transmembrane core and located in a mainly hydrophobic sub-pocket in proximity of Leu90, Leu91, Met177, Trp243, and Leu246. Superimposition of the family 1 docking conformations of each compound at the three hA_3AR models shows that the binding modes and the interactions are almost identical at the three binding sites (Fig. 4B). This data confirms the high conservation of residue orientation within the core region of the binding site of the three models.

The second set of conformations ('family 2' conformations, Fig. 5) presents the pyrazoloquinazoline moiety located approximately in the same position as family 1 conformations but with opposite orientation, hence presenting the 2-substituent pointed towards the extracellular region. Superimposition of the family 2 docking conformations of each compound at the three A_3AR models shows that there are some differences in compound orientation (Fig. 5B). In particular the 2-substituent results differently positioned at the three A_3AR models and this is due to only partial conservation of residue orientation at the extracellular region of the three models.

Considering both families of docking conformations, the 5-oxo-pyrazoloquinazoline derivatives herein reported form hydrophobic interactions with the hA_3 AR binding cleft, such as the π-stacking interaction between the compound scaffold and the Phe168 residue within the EL2 segment. In contrast, the double polar interaction of asparagine 6.55 amide group (Asn250) with both the NH_2 group and the N1 atom of ZM241385 (particularly evident in the 3EML crystal structure) is not observed for the 5-oxo pyrazoloquinazolines. It has to be noted that the asparagine residue 6.55, conserved among all ARs subtypes, was found to be important for ligand binding at both hA_3 and hA_{2A} ARs. Considering the family 1 conformations, the possible interactions of Asn250 with both the 5-oxo substituent and the N3 atom of the ligand is reduced to a single interaction. In fact, only a single H-bond link between the 5-oxo group or the 3-nitrogen atom and the Asn250 amine function is allowed, due also to the steric hindrance of the 2-aromatic ring that obstructs second possible interaction.

Replacement of the 2-aromatic substituent with an alkyl carboxylate group does not significantly improve the interaction with Asn250, hence suggesting the presence of an aromatic group in that compound position as structural requirement. In the case of family 2 conformations, a H-bond interaction is still observed between pyrazoloquinazoline derivatives and Asn250, and it is given by the 5-carbonyl group and the NH_2 segment of the asparagine amide moiety.

It must be underlined that the receptor affinity seems directly correlated to compound hydrophobicity. As a consequence, given the general pyrazoloquinazoline structure as constant, the different compound hydrophobicity is provided by the chemical–physical profile of 2-substituent. Considering its position within the binding pocket, it can be observed that family 1 conformations present this group inserted within TM3, TM5, and TM6 residues (Leu91, Thr94, Met177, Ser181, Ile186, Trp243, Ser247, and Asn250) in a sub-pocket characterized mainly by hydrophobic properties. The different chemical–physical profile of the 2-substituent could hence enhance or reduce the interaction with this sub-pocket. In the case of family 2 conformations, the 2-substituent is partially exposed to the extracellular environment. In this case the role of this substituent could be mainly related to its impact in compound solvation/desolvation, with the less water soluble compounds having higher affinity with respect to the more hydrophilic ones. These results are somehow confirmed by comparing the docking scores with the pK_i data. In fact, best matching between docking scores and binding affinity trends is given by two scoring functions of MOE, *dock-p*K_i and *Affinity dG* (Fig. 6). The first tool is based on an empirical scoring function consisting of a directional hydrogen-bonding term, a directional hydrophobic interaction term, and an entropic term (ligand rotatable bonds immobilized in binding). In particular the trend of the hydrophobic interaction term values for the top scoring pose of each compound present high correspondence with pK_i binding data tendency. The second scoring function shows significant correspondence with log*S* and log*P* data, hence highlighting the importance of compound solubility for receptor activity. It is important to point out that, in any case, if on one hand higher hydrophobicity is often correlated with higher binding activity, on the other hand hydrophobicity that is too high makes compounds difficult to be handle in experimental (and therapeutic) conditions. Log*P* analysis of all synthesized compounds shows that they all present predicted log*P* values <4, hence still in an acceptable range.

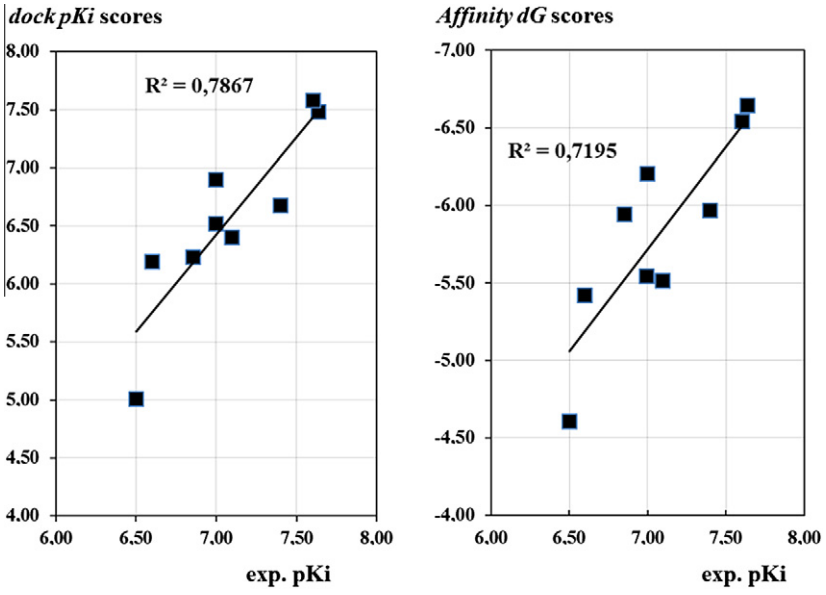

Figure 6. Comparison of docking scores with experimental binding data. Plots of *dock-p*K_i scores versus experimental pK_i data and *Affinity dG* scores versus experimental pK_i data from docking analysis at 3EML-based hA_3 AR model are shown.

A docking analysis was performed also to simulate the possible binding modes of simplified pyrazole derivatives **20–24** at hA_3AR binding site. The same docking and post-docking protocols were employed.

Due to their greater flexibility, these compounds present several combinations of conformation and orientation within the receptor binding site. Among them, two binding modes are particularly interesting due to their similarity with the above described family 1 and 2 docking conformations of pyrazoloquinazoline derivatives. The similarity is given in particular by a matching of the pyrazole ring of simplified and tricyclic compounds and a matching of the aromatic ring of the 2-aminophenyl group of pyrazole derivatives with the phenyl ring of the pyrazoloquinazoline scaffold, with the nitrogen atom of the free amino group of pyrazole derivatives being almost superimposed to the nitrogen atom at 6 position of the pyrazoloquinazoline scaffold (Fig. 7). Compounds **20** and **4** are shown as template for the pyrazole and tricyclic derivatives, respectively. The planarity of the simplified pyrazole derivatives is given by an internal H-bond interaction between the free amino group and one of the nitrogen atoms of the pyrazole scaffold. These compounds do not present the carbonyl group of the tricyclic derivatives hence the H-bond acceptor function interacting with Asn250 is missing. Therefore, while the planarity typical of AR antagonists is conserved, on the other hand the ability of the compound to give hydrophilic interactions with binding site residues is partially reduced with respect to the original tricyclic derivatives. Further optimization of these simplified derivatives could possibly restore the H-bonding ability.

5. Conclusion

The present study has led to the identification of some pyrazolo[1,5-*c*]quinazoline derivatives as hA_3 AR antagonists. In particular, the 5-oxo-substituted derivatives (series **B-1**) are endowed with good hA_3 receptor affinity and high selectivity, being totally inactive at all the other AR subtypes. In contrast, the corresponding 5-amino compounds (series **B-2**) do not bind or bind with very low affinity at the hA_3 AR the only exception being the 5-*N*-benzoyl derivative **19** that shows a hA_3 K_i value in the high μ-molar range. Moreover, the synthetic intermediates **20–24**, despite their simplified structure, possess the minimal molecular requirements for binding at the hA_3 AR, showing modest binding affinity for this receptor subtype but total selectivity versus all the other ARs. Molecular docking of tricyclic and simplified derivatives identified their hypothetical binding mode to our model of hA_3 receptor. As a new finding, the pyrazole derivatives emerged as lead candidates for the development of new monocyclic AR antagonists with improved physicochemical properties and, as a consequence, better bioavailability with respect to tricyclic compounds.

6. Experimental section

6.1. Chemistry

Silica gel plates (Merck F_{254}) and silica gel 60 (Merck; 70–230 mesh) were used for analytical and column chromatography, respectively. All melting points were determined on a Gallenkamp melting point apparatus. Microanalyses were performed with a Flash E1112 Thermofinnigan elemental analyzer for C, H, N, and the results were within ±0.4% of the theoretical values except where stated otherwise. The IR spectra were recorded with a Perkin–Elmer Spectrum RX I spectrometer in Nujol mulls and are expressed in cm^{-1}. The ^1H NMR spectra were obtained with a Bruker Avance 400 MHz instrument. The chemical shifts are reported in δ (ppm) and are relative to the central peak of the solvent. All the exchangeable protons were confirmed by addition of D_2O. The following abbreviations are used: s = singlet, d = doublet, dd = double doublet, t = triplet, m = multiplet, br = broad, ar = aromatic protons.

6.1.1. General method for the synthesis of 1-(hetero)aryl-3-(2-nitrophenyl)-2-propen-1-ones (26–28)

A solution of equimolar amounts (16 mmol) of 2-nitrobenzaldehyde and the suitable (etero)aryl methyl ketone in glacial acetic acid (8 mL) was treated with boron trifluoride acetic acid complex (48 mL). The reaction mixture was stirred at room temperature until the disappearance of the starting material (TLC monitoring). Saturated solution of sodium acetate (8 mL) and 20% NaOH solution were added to the resulting solution until pH 7 was reached. The solid which precipitates, was then collected by filtration and washed with water.

6.1.1.1. 1-(4-Methoxyphenyl)-3-(2-nitrophenyl)-2-propen-1-one (26)[26]. Yield: 78%, mp 112–114 °C (cyclohexane/EtOAc) (Lit. mp 93–94 °C from EtOH); ^1H NMR($CDCl_3$) δ 3.92 (s, 3H, OCH_3), 7.01 (d, 2H, ar, J = 8.95 Hz), 7.35 (d, 1H, H-2, J = 15.64 Hz), 7.58 (t, 1H, ar, J = 7.42 Hz), 7.70 (t, 1H ar, J = 7.42 Hz), 7.76 (d, 1H, ar, J = 7.42 Hz), 8.05 (d, 2H ar, J = 8.95 Hz), 8.09 (d, 1H, ar, J = 7.42 Hz), 8.15 (d, 1H, H-3, J = 15.64 Hz), IR: 1653, 1571, 1353. Anal. Calcd for $C_{16}H_{13}NO_4$: C, 67.84; H, 4.63; N, 4.94. Found C, 68.02; H, 4.39; N, 5.13.

6.1.1.2. 1-(2-Furyl)-3-(2-nitrophenyl)-2-propen-1-one (27)[27]. Column chromatography, eluting system cyclohexane/EtOAc 1:1; yield: 41%; mp 132–135 °C (EtOH); ^1H NMR (DMSO-d_6) δ 6.82–6.84 (m, 1H, ar), 7.69–7.74 (m, 2H, ar+H-2), 7.85 (t, 1H, ar, J = 7.60 Hz), 7.89 (d, 1H, ar, J = 3.56 Hz), 7.99 (d, 1H, H-3, J = 15.61 Hz), 8.10–8.16 (m, 3H, ar). IR: 1690, 1550, 1330. Anal. Calcd for $C_{13}H_9NO_4$: C, 64.20; H, 3.73; N, 5.76. Found C, 64.03; H, 3.98; N, 5.82.

6.1.1.3. 1-(2-Thienyl)-3-(2-nitrophenyl)-2-propen-1-one (28)[28]. Yield: 50%; mp 133–134 °C (EtOH) (Lit. mp 136 °C); ^1H NMR (DMSO-$\boldsymbol{d_6}$) δ: 7.35 (m, 1H, ar), 7.72 (t, 1H, ar, $\boldsymbol{J}$ = 8.36 Hz), 7.84–7.90 (m, ar+H-2), 7.99 (d, 1H, H-3, $\boldsymbol{J}$ = 15.49 Hz), 8.10–8.14 (m, 2H, ar), 8.20 (d, 1H, ar, $\boldsymbol{J}$ = 7.00 Hz), 8.38 (m, 1H, ar). IR: 1690, 1550, 1330. Anal. Calcd for $\boldsymbol{C_{13}H_9NO_3S}$: C, 60.22; H, 3.50; N, 5.40. Found C, 59.99; H, 3.29; N, 5.31.

6.1.2. General procedure for the synthesis of 4,5-dihydro-3-(hetero)aryl-5-(2-nitrophenyl)-1*H*-pyrazoles (29–31)

A solution of the suitable 1-(hetero)aryl-3-(2-nitrofenil)-2-propen-1-one **26**–**28** (6.7 mmol) and hydrazine hydrate (65%, 18.1 mmol) in EtOH (50 mL) was heated at reflux until the disappearance of the starting material (TLC monitoring). After cooling, a solid precipitated (compounds **29**, **31**) which was collected by filtration and washed with diethyl ether. A second crop of the desired compound was obtained after evaporation under reduced pressure of the mother ethanolic liquor and work-up with diethyl ether. The resulting crude product was purified by crystallization. In the case of compound **30**, the resulting solid was removed by filtration and the solvent was evaporated under reduced pressure. The residue was purified by column chromatography, eluting system methylene chloride/EtOAc 9:1, to yield a dark red oil which was the pure product.

6.1.2.1. 4,5-Dihydro-3-(4-methoxyphenyl)-5-(2-nitrophenyl)-1*H*-pyrazole (29). Yield: 88%; mp 72–73 °C (cyclohexane); ^1H NMR (DMSO-d_6) δ: ^1H NMR ($CDCl_3$) δ: 2.94 (dd, 1H, H-4, J = 16.6, 9.92 Hz), 3.73 (dd, 1H, H-4, J = 16.56, 10.80 Hz), 3.81 (s, 3H, OCH_3), 5.34 (t, 1H, H-5, J = 10.28 Hz), 6.14 (br s, 1H, NH), 6.88 (d, 2H, ar, J = 8.76 Hz), 7.41 (t, 1H, ar, J = 8.00 Hz), 7.58–7.62 (m, 3H,

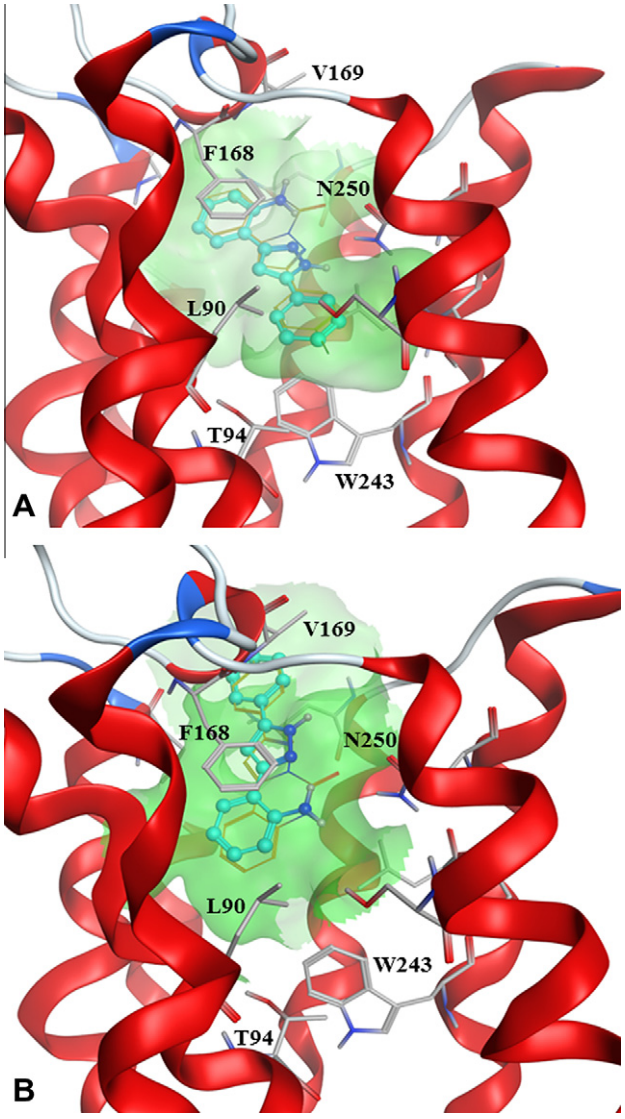

Figure 7. Docking conformations of simplified pyrazoles at 3EML-based hA_3AR model and comparison with family 1 (Panel A) and 2 (Panel B) docking conformations of pyrazoloquinazoline derivatives. Compounds **20** (ball and sticks, cyan) and **4** (line, yellow) are shown. Key receptor residues are indicated.

ar); 7.93 (m, 2H, ar); IR: 3353, 1515, 1463, 1341, 1250. Anal. Calcd for $C_{16}H_{15}N_3O_3$: C,64.64; H,5.09; N,14.13. Found C, 64.48; H, 4.89; N, 13.96.

6.1.2.2. 4,5-Dihydro-3-(2-furyl)-5-(2-nitrophenyl)-1*H*-pyrazole (30). Yield: 84%; (oil) ^{1}H NMR ($CDCl_3$) δ 2.99 (dd, 1H, H-4, J = 16.64, 9.8 Hz) 3.57 (dd, 1H, H-4, J = 16.52, 10.92 Hz), 5.42 (t, 1H, H-5, J = 10.36 Hz), 6.04 (s, 1H, NH), 6.48 (dd, 1H, ar, J = 3.40, 1.84 Hz), 6.58 (d, 1H, ar, J = 3.36 Hz), 7.47 (t, 1H, ar, J = 8.44 Hz), 7.51 (d, 1H, ar, J = 1.84 Hz), 7.67 (t, 1H, ar, J = 8.44 Hz), 7.95 (d, 1H, ar, J = 7.92 Hz), 8.01 (d, 1H, ar, J = 8.17 Hz); IR: 3300, 1650, 1550, 1340, 1250. Anal. Calcd for $C_{13}H_{11}N_3O_3$: C, 60.70; H, 4.31; N, 16.33. Found C, 60.58; H, 4.23; N, 16.17.

6.1.2.3. 4,5-Dihydro-5-(2-nitrophenyl)-3-(2-thienyl)-1*H*-pyrazole (31). Yield: 66%; mp 79–81 °C (MeOH); ^{1}H NMR (DMSO-d_6) δ 2.97 (dd, 1H, H-4, J = 16.52, 9.72), 3.62 (dd, 1H, H-4, 16.56, 11.08), 5.18 (td, 1H, H-5, J = 10.44, 3.56), 7.06 (dd, 1H, ar, J = 5.0, 3.64 Hz), 7.17 (d, 1H, ar, J = 4.28), 7.51–7.58 (m, 3H, ar+NH), 7.73–7.81 (m, 2H, ar), 7.99 (d, 1H, ar, J = 8.96 Hz); IR: 3340, 1654, 1540, 1338, 1251. Anal. Calcd for $C_{13}H_{11}N_3O_2S$: C, 57.13; H, 4.06; N,15.37. Found C, 57.08; H, 4.27; N, 15.09.

6.1.3. General procedure for the synthesis of 3(5)-(hetero)aryl-5(3)-(2-nitrophenyl)pyrazoles (32–34)

A solution of lead tetraacetate (3.74 mmol) in anhydrous dichloromethane (25 mL) was added dropwise to a solution of equimolar amount of **29**–**31** in anhydrous dichloromethane (25 mL). The addition of the oxidant agent was performed in about 20 min. The reaction mixture was stirred at room temperature for 15 min, and then, after addition of water (70 mL), a solid precipitated, which was removed by filtration. After separation of the resulting two layers, the organic solution was washed with water (50 mL × 3), anhydrified (Na_2SO_4) and evaporated under reduced pressure. The dark red oily residue was dissolved in a mixture of concentrated HCl (0.15 mL) and EtOH (20 mL) and heated at reflux for 30 min. The resulting solution was diluted with 2.5% $NaHCO_3$ and extracted with dichloromethane (50 mL). The organic layer was washed with water (50 mL × 3), anhydrified (Na_2SO_4) and evaporated under reduced pressure. The resulting crude product was purified by column chromatography, eluting system dichloromethane/EtOAc 9:1.

6.1.3.1. 3-(4-Methoxyphenyl)-5-(2-nitrophenyl)pyrazole (32). Yield: 60%; mp 148–149 °C (cyclohexane/EtOAc); ^{1}H NMR (DMSO-d_6) δ: 3.81 (s, 3H, OCH_3), 6.94 (s, 1H, pyrazole), 7.06 (d, 2H, ar, J = 8.56 Hz), 7.56 (t, 1H, ar, J = 7.56 Hz), 7.70–7.73 (m, 3H, ar), 7.81 (d, 1H, ar, J = 7.96 Hz), 7.85 (d, 1H, ar, J = 7.68 Hz), 13.48 (s, 1H, NH); IR: 3215, 1511, 1462. Anal. Calcd for $C_{16}H_{13}N_3O_3$: C, 65.08; H, 4.44; N, 14.23. Found C, 65.01; H, 4.57; N, 14.01.

6.1.3.2. 3-(2-Furyl)-5-(2-nitrophenyl)pyrazole (33)[21]. Yield: 44%; mp 121–123 °C (Lit. mp 121 °C dec) Anal. Calcd for $C_{13}H_9N_3O_3$ C, 61.18; H, 3.55; N, 16.46. Found C, 59.92; H, 3.29; N, 16.70.

6.1.3.3. 5-(2-Nitrophenyl)-3-(2-thienyl)pyrazole (34)[21]. Yield: 52%; mp 104–106 °C (Lit. mp 105–106 °C) C; Anal. Calcd for $C_{13}H_9N_3O_2S$: C, 57.55; H, 3.34; N, 15.49. Found C, 57.48; H, 3.08; N, 15.27.

6.1.4. General procedure for the synthesis of 3(5)-(hetero)aryl-5(3)-(2-aminophenyl)pyrazoles (21–23)

A mixture of **32**–**34** (1.7 mmol) and 30% (w/w) Pd/C (10%) in EtOAc (100 mL) was hydrogenated in a Parr apparatus at 30 psi until the disappearance of the starting material. Elimination of the catalyst and evaporation of the solvent at reduced pressure gave a solid which was purified by crystallization.

6.1.4.1. 5-(2-Aminophenyl)-3-(4-methoxyphenyl)pyrazole (21). Yield: 90%; mp 172–173 °C (toluene); ^{1}H NMR (DMSO-d_6) δ 3.81 (s, 3H, OCH_3), 6.35 (s, 2H, NH_2), 6.59 (t, 1H, ar, J = 7.32 Hz), 6.74 (d, 1H, ar, J = 8.00 Hz), 7.00 (t, 1H, ar, J = 7.68 Hz), 7.05–7.07 (m, 2H, ar+pyrazole), 7.57 (d, 1H, ar, J = 7.60 Hz), 7.76 (d, 2H, ar, J = 8.52 Hz), 13.15 (br s, 1H, NH); IR: 3363, 3291, 1610, 1459. Anal. Calcd for $C_{16}H_{15}N_3O$: C, 72.43; H, 5.70; N, 15.84. Found C, 72.31; H, 5.98; N, 16.02.

6.1.4.2. 5-(2-Aminophenyl)-3-(2-furyl)pyrazole (22)[21]. Yield: 90%; mp 127–128 °C (Lit. mp 127–128 °C). Anal. Calcd for $C_{13}H_{11}N_3O$: C, 69.32; H, 4.92; N, 18.66. Found C, 69.54; H, 5.11; N, 18.84.

6.1.4.3. 5-(2-aminophenyl)-3-(2-thienyl)pyrazole (23)[21]. Yield: 70%; mp 174–177 °C (Lit. mp 176–178 °C) Anal. Calcd for $C_{13}H_{11}N_3S$: C, 64.70; H, 4.59; N, 17.41. Found C, 64.53; H, 4.72; N, 17.19.

6.1.5. General procedure for the synthesis of 5,6-dihydro-2-(hetero)aryl-pyrazolo[1,5-*c*]quinazolin-5-ones (2, 6–7)

Triethylamine (3.36 mmol) and triphosgene (0.56 mmol) were successively added to a solution of **21**–**23** (1.4 mmol) in anhydrous tetrahydrofuran (10 mL). The reaction mixture was stirred at room temperature until the disappearance of the starting material and then diluted with water (30 mL). The resulting solid was collected by filtration and washed with water.

6.1.5.1. 5,6-Dihydro-2-(4-methoxyphenyl)pyrazolo[1,5-*c*]quinazolin-4-one (2). Yield: 88%; mp >300 °C (acetic acid); ^{1}H NMR (DMSO-d_6) δ: 3.84 (s, 3H, OCH_3), 7.09 (d, 2H, ar, J = 8.76 Hz), 7.31–7.36 (m, 2H, ar), 7.53 (t, 1H, ar, J = 7.07 Hz), 7.67 (s, 1H, pyrazole), 7.96 (d, 2H, ar, J = 8.72 Hz), 8.05 (d, 1H, ar, J = 7.84 Hz), 11.82 (s, 1H, NH); IR: 3197, 1725, 1682, 1453, 1376, 1254. Anal. Calcd for $C_{17}H_{13}N_3O_2$: C, 70.09; H, 4.50; N, 14.42. Found C, 69.81; H, 4.70; N, 14.01.

6.1.5.2. 5,6-Dihydro-2-(2-furyl)pyrazolo[1,5-*c*]quinazolin-4-one (6)[21]. Yield: 90%; mp 303–304 °C (acetic acid) (Lit. mp 304–305 °C); Anal. Calcd for $C_{14}H_9N_3O_2$: C, 66.93; H, 3.61; N, 16.73. Found C, 67.01; H, 3.41; N, 16.58.

6.1.5.3. 5,6-Dihydro-2-(2-thienyl)pyrazolo[1,5-*c*]quinazolin-4-one (7)[21]. Yield: 75%; mp 297–299 °C (acetic acid) (Lit. mp 299–300 °C); Anal. Calcd for $C_{14}H_9N_3OS$: C, 62.91; H, 3.39; N, 15.72. Found C, 63.12; H, 3.18; N, 15.98.

6.1.6. General procedure for the synthesis of 2-(hetero)aryl-pyrazolo[1,5-*c*]quinazolin-5-amines (15–18)

A solution of **20**–**23** (1.06 mmol), *para*-toluensulfonic acid (1.06 mmol) and an excess of cyanamide (6.12 mmol) in *N*-methyl-2-pyrrolidone (5 mL) was heated at reflux until the disappearance of the starting material (TLC monitoring). The reaction mixture was diluted with EtOAc (100 mL) and the resulting solid was eliminated by filtration. After concentration up to about 30 mL, the organic solution was washed with water (20 mL × 3) and anhydrified (Na_2SO_4). Evaporation of the solvent under reduced pressure gave a residue which was purified by silica gel column chromatography, eluting system cyclohexane/EtOAc 5:5 (compounds **15**–**16**) or $CHCl_3$/MeOH 9.5:0.5 (compounds **17**–**18**).

6.1.6.1. 2-Phenylpyrazolo[1,5-*c*]quinazolin-5-amine (15). Yield: 40%; mp 233–235 °C (EtOAc); ^{1}H NMR (DMSO-d_6) δ: 7.32 (t, 1H, ar, J = 7.35 Hz), 7.45–7.57 (m, 5H, ar), 7.60 (s, 2H, NH_2), 7.73 (s, 1H, pyrazole), 8.08–8.13 (m, 3H, ar); IR: 3450, 3405. Anal. Calcd for $C_{16}H_{12}N_4$: C, 73.83; H, 4.65; N, 21.52. Found C, 74.06; H, 4.81; N, 21.76.

6.1.6.2. 2-(4-Methoxyphenyl)-pyrazolo[1,5-*c*]quinazolin-5-amine (16). Yield: 87%; mp 243–244 °C (toluene); ^{1}H NMR (DMSO-d_6) δ: 3.84 (s, 3H, OCH_3), 7.09 (d, 2H, ar, J = 7.12 Hz), 7.30 (t, 1H, ar, J = 7.24 Hz), 7.47–7.55 (m, 4H, ar+NH_2), 7.62 (s, 1H, pyrazole), 8.03–8.07 (m, 3H, ar); IR: 3447, 1610, 1461. Anal. Calcd for $C_{17}H_{14}N_4O$: C, 70.33; H, 4.86; N, 19.30. Found C, 70.51; H, 5.01; N, 19.12.

6.1.6.3. 2-(2-Furyl)-pyrazolo[1,5-*c*]quinazolin-5-amine (17). Yield: 37%; mp 253–255 °C (EtOAc); ^{1}H NMR (DMSO-d_6) δ: 6.70–7.73 (m, 1H, ar), 7.08 (d, 1H, ar, J = 3.21 Hz), 7.33 (t, 1H, ar, J = 7.28 Hz), 7.49–7.58 (m, 3H, ar), 7.70 (s br, 2H, NH_2), 7.90 (s, 1H, pyrazole), 8.10 (d, 1H, ar, J = 7.56 Hz); IR: 3445, 3405, 1676. Anal. Calcd for $C_{14}H_{10}N_4O$: C, 67.19; H, 4.03; N, 22.39. Found C, 69.95; H, 3.86; N, 22.01.

6.1.6.4. 2-(2-Thienyl)-pyrazolo[1,5-*c*]quinazolin-5-amine (18). Yield: 71%; mp 170–171 °C (2-methoxyethanol); ^{1}H NMR (DMSO-d_6) δ: 7.22–7.24 (m, 1H, ar), 7.32 (t, 1H, ar, J = 7.40 Hz), 7.48–7.61 (m, 4H, ar+NH_2), 7.62 (s, 1H, pyrazole), 6.69 (d, 1H, ar, J = 4.88 Hz), 7.74 (d, 1H, ar, J = 3.48 Hz), 8.07 (d, 1H, ar J = 7.68 Hz); IR: 3441, 1462. Anal. Calcd for $C_{14}H_{10}N_4S$: C, 63.14; H, 3.78; N, 21.04. Found C, 62.99; H, 4.01; N, 20.88.

6.1.7. 2-Phenylpyrazolo[1,5-*c*]quinazolin-5-benzamide (19)

A solution of benzoyl chloride (3 mmol) in anhydrous dichloromethane (5 mL) was dropwise added to a cold (0 °C) suspension of **15** (1 mmol) in anhydrous dichloromethane (30 mL) and pyridine (10 mmol). The reaction mixture was stirred at room temperature for 12 h. The resulting solution was washed with water (30 mL × 3), anhydrified (Na_2SO_4) and evaporated under reduced pressure to yield a red oily residue which was purified by silica gel column chromatography, eluting system cyclohexane/EtOAc 6:4. Yield: 33%; mp 178–180 °C (EtOH); ^{1}H NMR (DMSO-d_6) δ: 7.46 (t, 1H, ar, J = 7.28 Hz), 7.53 (t, 2H, ar, J = 7.38 Hz), 7.60–7.79 (m, 5H, ar), 7.86 (d, 1H, ar, J = 7.88 Hz), 7.96 (s, 1H, pyrazole), 8.06 (d, 2H, ar, J = 7.12 Hz), 8.13–8.16 (m, 2H, ar), 8.30 (d, 2H, ar, J = 7.81 Hz), 11.29 (s, 1H, NH); IR: 3350, 1632. Anal. Calcd for $C_{23}H_{16}N_4O$: C, 75.81; H, 4.43; N, 15.38. Found C, 76.00; H, 4.21; N, 15.60.

6.1.8. 5,6-Dihydro-5-oxo-pyrazolo[1,5-*c*]quinazolin-2-carboxylic acid (35)[21]

A suspension of **10**[20] (6.64 mmol) in a mixture of glacial acetic acid (26 mL) and 6 N HCl (5 mL) was heated at reflux for 30 h. After cooling a solid precipitated which was collected by filtration and washed with water. Yield: 91%; mp 283 °C dec (acetic acid/H_2O) (Lit. mp 282 °C dec). Anal. Calcd for $C_{11}H_7N_3O_3$: C, 57.65; H, 3.08; N, 18.33. Found C, 57.80; H, 3.00; N, 18.25.

6.1.9. Benzyl 5,6-dihydro-5-oxo-pyrazolo[1,5-*c*]quinazolin-2-carboxylate (12)

A suspension of **35** (1.74 mmol) in thionyl chloride (20 mL) was heated at reflux for 4 h. After evaporation at reduced pressure of the excess of thionyl chloride, the last traces of the chlorinating agent were removed by repeated treatment of the resulting residue with cyclohexane (30 mL × 3) and subsequent distillation of the solvent. A suspension of the crude 5,6-dihydro-5-oxo-pyrazolo[1,5-*c*]quinazolin-2-carbonyl chloride in tetrahydrofuran (50 mL) and benzyl alcohol (23 mL) was heated at reflux for 7 h. Elimination of the solvent by evaporation at reduced pressure gave a solid which was dissolved in EtOAc (70 mL). The organic layer was washed with water (40 mL × 4) and anhydrified (Na_2SO_4). Evaporation of the solvent under reduced pressure gave an oily residue which solidified after treatment with EtOH. Yield: 43%; mp 270–272 °C (2-methoxyethanol); ^{1}H NMR (DMSO-d_6) δ: 5.43 (s, 2H, CH_2), 7.29–7.46 (m, 5H, ar), 7.51–7.57 (m, 3H, ar), 7.75 (s, 1H, pyrazole), 8.17 (d, 1H, ar, J = 7.84 Hz), 12.12 (s, 1H, NH); IR: 3232, 1733, 1710. Anal. Calcd for $C_{18}H_{13}N_3O_3$: C, 67.71; H, 4.10; N, 13.16. Found C, 67.49; H, 4.29; N, 13.00.

6.1.10. 5,6-Dihydro-5-oxo-pyrazolo[1,5-*c*]quinazolin-2-benzylcarboxamide (13)

A solution of **35** (1.74 mmol), benzylamine (2.60 mmol), *N*-(3-dimethylaminopropyl)-*N*′-ethylcarbodiimide hydrochloride (1,74 mmol) and 1-hydroxybenzotriazole hydrate (2 mmol) in anhydrous dimethylformamide (33 mL) was heated at reflux for 5 h. After cooling the resulting solution was diluted with water (70 mL) and the resulting solid was collected by filtration and washed with water. Yield: 52%; mp >300 °C (2-methoxyethanol); ^{1}H NMR (DMSO-d_6) δ: 4.49 (d, 2H, CH_2, J = 6.28 Hz), 7.23–7.26 (m, 1H, ar), 7.30–7.38 (m, 6H, ar), 7.55 (t, 1H, ar, J = 7.24 Hz),

7.61 (s, 1H, pyrazole), 8.14 (d, 1H, ar, J = 7.16 Hz), 9.24 (t, 1H, NH, J = 6.20 Hz), 12.01 (s br, 1H, NH); IR: 339, 3111, 1732. Anal. Calcd for $C_{18}H_{14}N_4O_2$: C, 67.91; H, 4.43; N, 17.60. Found C, 68.08; H, 4.15; N, 17.90.

6.2. Computational methodologies

All molecular modeling studies were performed on a 2 CPU (PIV 2.0-3.0 GHZ) Linux PC. Homology modeling, energy minimization, and docking studies were carried out using Molecular Operating Environment (MOE, version 2010.10) suite. All ligand structures were optimized using RHF/AM1 semi-empirical calculations and the software package MOPAC implemented in MOE was utilized for these calculations.

6.2.1. Homology modeling of the human A_3AR

Homology models of the hA_3AR were built using recently solved X-ray structures of the $hA_{2A}AR$ in complex with ZM241385 as templates (pdb code: 3EML; 2.6-Å resolution;[29] PDB code: 3PWH; 3.3-Å resolution;[30] PDB code: 3VG9; 2.7-Å resolution[31]). A multiple alignment of the AR primary sequences was built within MOE as preliminary step. For all hA_3AR models, the boundaries identified from the utilized X-ray crystal structure of $hA_{2A}AR$ were then applied for the corresponding sequences of the TM helices of the hA_3AR. The missing loop domains were built by the loop search method implemented in MOE. Once the heavy atoms were modeled, all hydrogen atoms were added, and the protein coordinates were then minimized with MOE using the AMBER99 force field.[36] The minimizations were performed by 1000 steps of steepest descent followed by conjugate gradient minimization until the RMS gradient of the potential energy was less than 0.05 kJ mol^{-1} Å^{-1}. Reliability and quality of these models were checked using the Protein Geometry Monitor application within MOE, which provides a variety of stereochemical measurements for inspection of the structural quality in a given protein, like backbone bond lengths, angles and dihedrals, Ramachandran φ–ψ dihedral plots, and side-chain rotamer and nonbonded contact quality.

6.2.2. Molecular docking analysis

All compound structures were docked into the binding site of the three hA_3AR models using the MOE Dock tool. This method is divided into a number of stages. *Conformational analysis of ligands*: The algorithm generated conformations from a single 3D conformation by conducting a systematic search. In this way, all combinations of angles were created for each ligand. *Placement*: A collection of poses was generated from the pool of ligand conformations using Triangle Matcher placement method. Poses were generated by superposition of ligand atom triplets and triplet points in the receptor binding site. The receptor site points are alpha sphere centers which represent locations of tight packing. At each iteration a random conformation was selected, a random triplet of ligand atoms and a random triplet of alpha sphere centers were used to determine the pose. *Scoring*: Poses generated by the placement methodology were scored using two available methods implemented in MOE, the *London dG* scoring function which estimates the free energy of binding of the ligand from a given pose, and *Affinity dG* scoring which estimates the enthalpic contribution to the free energy of binding. The top 30 poses for each ligand were output in a MOE database.

6.2.3. Post docking analysis

The five top-score docking poses of each compound were then subjected to AMBER99 force field energy minimization until the RMS gradient of the potential energy was less than 0.05 kJ mol^{-1} Å^{-1}. Receptor residues within 6 Å distance from the ligand were left free to move, while the remaining receptor coordinates were kept fixed. AMBER99 partial charges of receptor and MOPAC output partial charges of ligands were utilized. Once the compound-binding site energy minimization was completed, receptor coordinates were fixed and a second energy minimization stage was performed leaving free to move only compound atoms. MMFF94[37–43]force field was applied. For each compound, the minimized docking poses were then rescored using *London dG* and *Affinity dG* scoring functions and the *dock-pK_i* predictor. The latter tool allows estimation of the pK_i for each ligand using the 'scoring.svl' script retrievable at the SVL exchange service (Chemical Computing Group, Inc. SVL exchange: http://svl.chemcomp.com). The algorithm is based on an empirical scoring function consisting of a directional hydrogen-bonding term, a directional hydrophobic interaction term, and an entropic term (ligand rotatable bonds immobilized in binding). For each compound, the three top-score docking poses according to at least two out of three scoring functions were selected for final ligand–target interaction analysis.

6.3. Pharmacology

6.3.1. Human cloned A_1, A_{2A} and A_3 AR binding assay

All synthesized compounds were tested to evaluate their affinity at hA_1, hA_{2A} and hA_3 adenosine receptors. Displacement experiments of [^{3}H]DPCPX (1 nM) to hA_1 CHO membranes (50 μg of protein/assay) and at least six to eight different concentrations of antagonists for 120 min at 25 °C in 50 mM Tris HCl buffer pH 7.4 were performed.[44] Non specific binding was determined in the presence of 1 μM of DPCPX (⩽10% of the total binding). Binding of [^{3}H]ZM-241385 (1 nM) to hA_{2A}CHO membranes (50 μg of protein/assay) was performed using 50 mM Tris HCl buffer, 10 mM $MgCl_2$ pH 7.4 and at least six to eight different concentrations of antagonists studied for an incubation time of 60 min at 4 °C.[45] Non specific binding was determined in the presence of 1 μM ZM241385 and was about 20% of total binding. Competition binding experiments to hA_3 CHO membranes (50 μg of protein/assay) and 0.5 nM [^{125}I]AB-MECA, 50 mM Tris HCl buffer, 10 mM $MgCl_2$, 1 mM EDTA, pH 7.4, were conducted, and at least six to eight different concentrations of examined ligands for 120 min at 4 °C.[46] Non specific binding was defined as binding in the presence of 1 μM AB-MECA and was about 20% of total binding. Bound and free radioactivity were separated by filtering the assay mixture through Whatman GF/B glass fiber filters using a Brandel cell harvester. The filter bound radioactivity was counted by Scintillation Counter Packard Tri Carb 2810 TR with an efficiency of 62%.

6.3.2. Measurement of cyclic AMP levels in CHO cells transfected with hA_{2B} or hA_3 ARs

CHO cells transfected with hAR subtypes were washed with phosphate-buffered saline, diluted tripsine and centrifuged for 10 min at 200 g. The pellet containing the CHO cells (1×10^6 cells/assay) was suspended in 0.5 ml of incubation mixture (mM): NaCl 15, KCl 0.27, NaH_2PO_4 0.037, $MgSO_4$ 0.1, $CaCl_2$ 0.1, Hepes 0.01, $MgCl_2$ 1, glucose 0.5, pH 7.4 at 37 °C, 2 IU/ml adenosine deaminase and 4-(3-butoxy-4-methoxybenzyl)-2-imidazolidinone (Ro 20-1724) as phosphodiesterase inhibitor and preincubated for 10 min in a shaking bath at 37 °C. The potency of antagonists to A_{2B} ARs was determined by antagonism of NECA (200 nM)-induced stimulation of cyclic AMP levels. In addition, the potency of antagonists to A_3 receptors was determined in the presence of forskolin 1 μM and Cl-IB-MECA (100 nM) that mediated inhibition of cyclic AMP levels. The reaction was terminated by the addition of cold 6% trichloroacetic acid (TCA). The TCA suspension was centrifuged at 2000 g for 10 min at 4 °C and the supernatant was extracted four times with water saturated diethyl ether. The final aqueous solution was tested for cyclic AMP levels by a competition protein binding assay. Samples of cyclic AMP standard (0–10

pmoles) were added to each test tube containing [^{3}H] cyclic AMP and the incubation buffer (trizma base 0.1 M, aminophylline 8.0 mM, 2-mercaptoethanol 6.0 mM, pH 7.4). The binding protein prepared from beef adrenals, was added to the samples previously incubated at 4 °C for 150 min, and after the addition of charcoal were centrifuged at 2000 g for 10 min. The clear supernatant was counted in a Scintillation Counter Packard Tri Carb 2500 TR with an efficiency of 58%.[47]

6.3.3. Data analysis

The protein concentration was determined according to a Bio-Rad method[48] with bovine albumin as a standard reference. Inhibitory binding constant (K_i) values were calculated from those of IC_{50} according to Cheng & Prusoff equation $K_i = IC_{50}/(1 + [C^*]/K_D^*)$, where $[C^*]$ is the concentration of the radioligand and K_D^* its dissociation constant.[49] A weighted non linear least-squares curve fitting program LIGAND[50] was used for computer analysis of inhibition experiments. EC_{50} and IC_{50} values obtained in cyclic AMP assay were calculated by non linear regression analysis using the equation for a sigmoid concentration-response curve (GraphPAD Prism, San Diego, CA, USA).

Acknowledgment

This work was supported by a Grant from the Italian Ministry for University and research (MIUR, FIRB RBNE03YA3L project).

References and notes

1. Fredholm, B. B.; IJzerman, A. P.; Jacobson, K. A.; Klotz, K. N.; Linden, J. *Pharmacol. Rev.* **2001**, *53*, 527.
2. Jacobson, K. A.; Knutsen, L. J. S. In *Handbook of Experimental Pharmacology, Purinergic and Pyrimidinergic Signalling I*; Abbracchio, M. P., Williams, M., Eds.; Springer: Berlin, 2001; Vol. 151, p 129.
3. Ralevic, V.; Burnstock, G. *Pharmacol. Rev.* **1998**, *50*, 413.
4. Jacobson, K. A.; Gao, Z. G. *Nat. Rev. Drug Disc.* **2006**, *5*, 247.
5. Pugliese, A. M.; Coppi, E.; Volpini, R.; Cristalli, G.; Corradetti, R.; Jeong, L. S.; Jacobson, K. A.; Pedata, F. *Biochem. Pharmacol.* **2007**, *74*, 768.
6. Colotta, V.; Catarzi, D.; Varano, F.; Capelli, F.; Lenzi, O.; Filacchioni, G.; Martini, C.; Trincavelli, L.; Ciampi, O.; Pugliese, A. M.; Pedata, F.; Schiesaro, A.; Morizzo, E.; Moro, S. *J. Med. Chem.* **2007**, *50*, 4061.
7. Gessi, S.; Merighi, S.; Varani, K.; Leung, E.; Mac Lennan, S.; Borea, P. A. *Pharmacol. Ther.* **2008**, *117*, 123.
8. Merighi, S.; Mirandola, P.; Varani, K.; Gessi, S.; Leung, E.; Baraldi, P. G.; Tabrizi, M. A.; Borea, P. A. *Pharmacol. Ther.* **2003**, *100*, 31.
9. Lenzi, O.; Colotta, V.; Catarzi, D.; Varano, F.; Filacchioni, G.; Martini, C.; Trincavelli, L.; Ciampi, O.; Varani, K.; Marighetti, F.; Morizzo, E.; Moro, S. *J. Med. Chem.* **2006**, *49*, 3916.
10. Colotta, V.; Catarzi, D.; Varano, F.; Lenzi, O.; Filacchioni, G.; Martini, C.; Trincavelli, L.; Ciampi, O.; Traini, C.; Pugliese, A. M.; Pedata, F.; Morizzo, E.; Moro, S. *Bioorg. Med. Chem.* **2008**, *16*, 6086.
11. Colotta, V.; Lenzi, O.; Catarzi, D.; Varano, F.; Filacchioni, G.; Martini, C.; Trincavelli, L.; Ciampi, O.; Pugliese, A. M.; Traini, C.; Pedata, F.; Morizzo, E.; Moro, S. *J. Med. Chem.* **2009**, *52*, 2407.
12. Colotta, V.; Catarzi, D.; Varano, F.; Cecchi, L.; Filacchioni, G.; Martini, C.; Trincavelli, L.; Lucacchini, A. *J. Med. Chem.* **2000**, *43*, 3118.
13. Colotta, V.; Capelli, F.; Lenzi, O.; Catarzi, D.; Varano, F.; Poli, D.; Vincenzi, F.; Varani, K.; Borea, P. A.; Dal Ben, D.; Volpini, R.; Cristalli, G.; Filacchioni, G. *Bioorg. Med. Chem.* **2009**, *17*, 401.
14. Lenzi, O.; Colotta, V.; Catarzi, D.; Varano, F.; Squarcialupi, L.; Filacchioni, G.; Varani, K.; Vincenzi, F.; Borea, P. A.; Dal Ben, D.; Lambertucci, C.; Cristalli, G. *Bioorg. Med. Chem.* **2011**, *19*, 3757.
15. Catarzi, D.; Colotta, V.; Varano, F.; Calabri, F. R.; Lenzi, O.; Filacchioni, G.; Trincavelli, L.; Martini, C.; Tralli, A.; Monopoli, C.; Moro, S. *Bioorg. Med. Chem.* **2005**, *13*, 705.
16. Catarzi, D.; Colotta, V.; Varano, F.; Lenzi, O.; Filacchioni, G.; Trincavelli, L.; Martini, C.; Montopoli, C.; Moro, S. *J. Med. Chem.* **2005**, *48*, 7932.
17. Morizzo, E.; Capelli, F.; Lenzi, O.; Catarzi, D.; Varano, F.; Filacchioni, G.; Vincenzi, F.; Varani, K.; Borea, P. A.; Colotta, V.; Moro, S. *J. Med. Chem.* **2007**, *50*, 6596.
18. Lenzi, O.; Colotta, V.; Catarzi, D.; Varano, F.; Poli, D.; Filacchioni, G.; Varani, K.; Vincenzi, F.; Borea, P. A.; Paoletta, S.; Morizzo, E.; Moro, S. *J. Med. Chem.* **2009**, *52*, 7640.
19. Poli, D.; Catarzi, D.; Colotta, V.; Varano, F.; Filacchioni, G.; Daniele, S.; Trincavelli, L.; Martini, C.; Paoletta, S.; Moro, S. *J. Med. Chem.* **2011**, *54*, 2102.
20. Colotta, V.; Catarzi, D.; Varano, F.; Melani, F.; Filacchioni, G.; Cecchi, L.; Galli, A.; Costagli, C. *Il Farmaco* **1996**, *51*, 223.
21. Colotta, V.; Catarzi, D.; Varano, F.; Filacchioni, G.; Cecchi, L.; Galli, A.; Costagli, C. *J. Med. Chem.* **1996**, *39*, 2915.
22. Jung, K. Y.; Kim, S. K.; Gao, Z. G.; Gross, A. S.; Melman, N.; Jacobson, J. A.; Kim, Y. C. *Bioorg. Med. Chem.* **2004**, *12*, 613.
23. Alanine, A.; Anselm, L.; Steward, L.; Thomi, S.; Vifian, W.; Groaning, M. D. *Bioorg. Med. Chem. Lett.* **2004**, *14*, 817.
24. Varano, F.; Catarzi, D.; Colotta, V.; Cecchi, L.; Filacchioni, G.; Galli, A.; Costagli, C. *Arch. Pharm. Pharm. Med. Chem.* **1996**, *329*, 529.
25. Varano, F.; Catarzi, D.; Colotta, V.; Calabri, F. R.; Lenzi, O.; Filacchioni, G.; Galli, A.; Costagli, C.; Deflorian, F.; Moro, S. *Bioorg. Med. Chem.* **2005**, *13*, 5536.
26. Barros, A. I. R. N. A.; Dias, A. F. R.; Silva, A. M. S. *Monatshefte für Chemie* **2007**, *138*, 585.
27. Nepali, K.; Singh, G.; Turan, A.; Agarwal, A.; Sapra, S.; Kumar, R.; Banerjee, U. C.; Verma, P. K.; Satti, N. K.; Gupta, M. K.; Suri, O. P.; Dhar, K. L. *Bioorg. Med. Chem.* **2011**, *19*, 1950.
28. Kushawaha, S. *J. Indian Chem. Soc.* **1968**, *45*, 752.
29. Jaakola, V. P.; Griffith, M. T.; Hanson, M. A.; Cherezov, V.; Chien, E. Y.; Lane, J. R.; Ijzerman, A. P.; Stevens, R. C. *Science* **2008**, *322*, 1211.
30. Doré, A. S.; Robertson, N.; Errey, J. C.; Ng, I.; Hollenstein, K.; Tehan, B.; Hurrell, E.; Bennett, K.; Congreve, M.; Magnani, F.; Tate, C. G.; Weir, M.; Marshall, F. H. *Structure* **2011**, *19*, 1283.
31. Hino, T.; Arakawa, T.; Iwanari, H.; Yurugi-Kobayashi, T.; Ikeda-Suno, C.; Nakada-Nakura, Y.; Kusano-Arai, O.; Weyand, S.; Shimamura, T.; Nomura, N.; Cameron, A. D.; Kobayashi, T.; Hamakubo, T.; Iwata, S.; Murata, T. *Nature* **2012**, *482*, 237.
32. Dal Ben, D.; Lambertucci, C.; Marucci, G.; Volpini, R.; Cristalli, G. *Curr. Top. Med. Chem.* **2010**, *10*, 993.
33. Costanzi, S.; Ivanov, A. A.; Tikhonova, I. G.; Jacobson, K. A. *Front. Drug Des. Discov.* **2007**, *3*, 63.
34. Molecular Operating Environment; C.C.G., Inc., 1255 University St., Suite 1600, Montreal, Quebec, Canada H3B 3X3.
35. Stewart, J. J. *J. Comput. Aided Mol. Des.* **1990**, *4*, 1.
36. Cornell, W. D.; Cieplak, P.; Bayly, C. I.; Gould, I. R.; Merz, K. M.; Ferguson, D. M.; Spellmeyer, D. C.; Fox, T.; Caldwell, J. W.; Kollman, P. A. *J. Am. Chem. Soc.* **1995**, *117*, 5179.
37. Halgren, T. A. *J. Comput. Chem.* **1996**, *17*, 490.
38. Halgren, T. A. *J. Comput. Chem.* **1996**, *17*, 520.
39. Halgren, T. A. *J. Comput. Chem.* **1996**, *17*, 553.
40. Halgren, T. A. *J. Comput. Chem.* **1996**, *17*, 587.
41. Halgren, T. A.; Nachbar, R. *J. Comput. Chem.* **1996**, *17*, 616.
42. Halgren, T. A. *J. Comput. Chem.* **1999**, *20*, 720.
43. Halgren, T. A. *J. Comput. Chem.* **1999**, *20*, 730.
44. Borea, P. A.; Dalpiaz, A.; Varani, K.; Gessi, S.; Gilli, G. *Life Sci.* **1996**, *59*, 1373.
45. Varani, K.; Rigamonti, D.; Sipione, S.; Camurri, A.; Borea, P. A.; Cattabeni, F.; Abbracchio, M. P.; Cattaneo, E. *FASEB J.* **2001**, *15*, 1245.
46. Varani, K.; Cacciari, B.; Baraldi, P. G.; Dionisotti, S.; Ongini, E.; Borea, P. A. *Life Sci.* **1998**, *63*, PL 81.
47. Varani, K.; Gessi, S.; Merighi, S.; Vincenzi, F.; Cattabriga, E.; Benini, A.; Klotz, K.-N.; Baraldi, P. G.; Tabrizi, M.-A.; Mac Lennan, S.; Leung, E.; Borea, P. A. *Biochem. Pharmacol.* **2005**, *70*, 1601.
48. Bradford, M. M. *Anal. Biochem.* **1976**, *72*, 248.
49. Cheng, Y. C.; Prusoff, W. H. *Biochem. Pharmacol.* **1973**, *22*, 3099.
50. Munson, P. J.; Rodbard, D. *Anal. Biochem.* **1980**, *107*, 220.